Progress In Electromagnetics Research, Vol. 127, 427–444, 2012

UTILIZATION OF SCREEN PRINTED LOW CURING TEMPERATURE COBALT NANOPARTICLE INK FOR MINIATURIZATION OF PATCH ANTENNAS

M. Nelo*, A. K. Sowpati, V. K. Palukuru, J. Juuti, and H. Jantunen

Microelectronics and Materials Physics Laboratories, University of Oulu, P. O. Box 4500, FI-90014, Finland

Abstract—This investigation is one of the first steps towards the realization of low-cost, mass producible, miniaturized antenna solutions utilizing screen printed magnetic thick films of cobalt nanoparticle ink. The ink has a curing temperature lower than 125°C, feasible printing characteristics and metal loading higher than 85 wt.%. The properties are achieved by using an oxidatively polymerising natural fatty acid, linoleic acid, both as a surfactant and a binder. DSC-TGA-MS-analysis, TEM and SEM microscopies were utilized to investigate ink composition, nanoparticle coating and print quality. The resonant frequency of a microstrip patch antenna was tuned by screen printing of cobalt nanoparticle ink with different layer thicknesses on top of the antenna element. The influence of magnetic layers on resonance frequency, return loss, total efficiency and radiation pattern was measured and compared with a reference antenna without the magnetic films. For example, five layers of magnetic film (52 μm total thickness) tuned the resonance frequency (2.49 GHz) of the patch antenna by 68 MHz. The radiation efficiency of the patch antenna was increased from 39% to 43% by the loading of a 52 μm thick magnetic film compared to the reference antenna. The radiation patterns remained essentially unchanged, despite the presence of the magnetic thick films.

Received 14 March 2012, Accepted 9 April 2012, Scheduled 27 April 2012

* Corresponding author: Mikko Nelo (mikko.nelo@ee.oulu.fi).

1. INTRODUCTION

In the era of modern wireless communications, antennas with small size, light weight and ease of fabrication are highly desired. Beside the requirement of miniaturization, other parameters such as bandwidth, radiation efficiency and antenna gain are also important for reliable telecommunication devices. In most cases, antenna size can be greatly reduced by using a substrate with high relative permittivity [1, 2]. However, this approach has given rise to decreased bandwidth and excitation of surface waves, leading to lower radiation efficiencies. A thicker substrate can be used to increase the bandwidth of the patch, but it will suffer from increased surface excitation, which will lower the efficiency [3]. The use of materials with relative permeability (μ_r) greater than one can also lead to antenna miniaturization in addition to enhanced bandwidths, tunable operation frequency, polarization diversity and beam steering [4–7]. Bulk ferrite materials [6], composites of ferrite particles in a polymer matrix [8] and metamaterials with embedded metallic circuits [9] have all been used as antenna substrates to achieve $\mu_r > 1$. However, they are too lossy to be used at frequencies > 600 MHz under self-bias condition, i.e., where no bias magnetic field is needed.

Self-biased magnetic materials are found to be useful for miniaturization of antenna substrates in applications such as hand held wireless communication devices. However, it has been challenging to synthesize self-biased magnetic antenna substrate materials for the frequencies above 600 MHz due to the well-known Snoek limit [10]. Recently, magnetic thin films have shown an ability to overcome this problem, obtaining μ_r greater than one [11–13] and operating frequencies > 1 GHz. Self-biased magnetization with high ferromagnetic resonant frequencies (FMR) up to several GHz are achieved by the strong demagnetization fields of magnetic films. This property is necessary for microwave devices [12, 13]. In the literature, ferromagnetic thin films have been utilized in order to tune the operating frequency of a patch antenna [6, 7, 11, 13], and to obtain enhanced bandwidth [11] and increased gain [13].

However, expensive fabrication methods in the realization of magnetic thin films, such as sputtering, have limited the use of such magnetic thin films in the mass-production of low cost microwave devices. In order to realize these devices in a cost effective manner different manufacturing methods should be utilized. In this case, screen printing was selected for applying the magnetic material. In order to obtain feasible microwave characteristics and maintain reasonable material costs, commercial solid cobalt nanoparticles were chosen as

raw materials for the ink development.

Fatty acids are relatively common materials in the stabilization of nanoparticle inks. This is due to their utility both as a capping molecule during nanoparticle synthesis [14] and as a stabilizing agent in the nanoparticle suspensions [15, 16]. In addition, unsaturated fatty acids have the capability of reacting into cross-linked polymeric structures when exposed to oxygen [17]. Their carboxylic acid group can also make a covalent bond to metallic surfaces (such as copper antenna patterns). These properties combined make them useful both as surfactants and binding materials.

Magnetic nanoparticles are useful in various applications including electromagnetic devices [18], high-density storage media [19, 20], ferrofluids [21], magnetic resonant imaging [22], drug delivery [23], and catalysts [24]. Magnetic metallic cobalt nanoparticles offer an interesting option as a raw material because using solid nanoparticles as a starting point instead of synthesizing them *in situ* simplifies the process substantially. The key issue in the use of dry nanoparticles is finding a way of stabilizing the particles into a suspension.

Biphase formulation of monolayers from stabilized cobalt nanoparticle suspensions has been studied [25, 26], as well as formulation of cobalt nanoparticle suspensions by precipitation of cobalt salts into metallic nanoparticles sterically protected by a layer of surfactant [27]. These methods incorporate the synthesis of cobalt nanoparticles which makes the process more complex and expensive for industrial scale production. Recently, the first research into the formulation of stable cobalt nanoparticle inks by using dry cobalt nanoparticles reacted with surfactant was reported by Nelo et al. [28].

In this work, linoleic acid was used simultaneously as surfactant and binder for screen printable ink. Patch antennas were loaded with screen printed magnetic thick films containing 85 wt.% of cobalt nanoparticles. The effects of the printed magnetic film on antenna performance were measured and compared to those found in reference antennas without magnetic material. The presence of magnetic films tuned the operating frequencies of the antennas remarkably and increased their efficiency. This is further analyzed and discussed.

2. EXPERIMENTAL DETAILS

2.1. Fabrication and Characterization of Magnetic Ink

The nanoparticles used were 28 nm cobalt nanoparticles produced by Nanostructured & Amorphous Materials Inc, (Los Alamos, USA). They contained 99.8 wt.% cobalt and were partially passivated with oxygen by the manufacturer. The specific surface area of the

nanopowder was determined with Brunauer-Emmett-Teller (BET) surface area analysis based on the physical adsorption of nitrogen gas. The measurement was made with a Micromeritics ASAP 2020 (Micromeritics Instrument Corporation, USA) and the specific surface area was 17.3 m^2/g. Linoleic acid with a purity of > 99% was purchased from Sigma-Aldrich, Germany. Solvents used were terpineol (> 99%. Merck, Germany) and Aa-grade ethanol (99.5%, Altia, Finland).

The required amount of linoleic acid for surface coating of the particles was calculated on the basis of the specific surface area of the powder. Since the area occupied by one carboxylic acid group on the surface of the particles is constant (0.21 nm^2) [29], the consumption of fatty acid for coating of the particles can be calculated on the basis of the molar mass of linoleic acid, resulting to need of 1.9 g of the acid for 50 g of nanoparticles. In addition to the calculated value, 5.3 g of linoleic acid was added to improve the ink's rheological properties during printing and to act as a binding material on the metal surfaces. The additional amount of fatty acid was decided on the basis of printing experiments.

Linoleic acid was dissolved in 100 ml of ethanol after which 50.0 g of dry particles were added into the resulting solution. Suspension was homogenized with ultrasonic agitation (Hielscher UP 100H, Hielscher, Germany) at 30 watts for 30 seconds. The suspension was then milled in a ball mill using a nylon cup and agate milling balls at moderate speed for 16 hours in order to break the agglomerates formed by the nanoparticles. After milling, the solvent was evaporated at 90°C for 16 hours in a nitrogen atmosphere in order to avoid oxidative polymerization of the surfactant. The dried particles were collected and mixed with terpineol using an agate mortar in order to obtain a smooth and homogenous printing ink. A sample was set aside for gravimetric analysis. The inorganic and organic solids and volatiles of the sample were measured with a Netzsch STA 409PC thermogravimetry-differential scanning calorimetry-mass spectrometer (TGA-DSC-MS) analyzer in a helium atmosphere in order to avoid oxidative reactions (NETZSCH-Geraetebau GmbH, Germany).

The nanoparticles were analyzed with a LEO 912 OMEGA analytical energy-filtered transmission electron microscope (EFTEM) (Carl Zeiss SMT AG, Germany) to observe the layers of fatty acid surfactant on top of the particles. First, 0.2 g of surface treated particles were washed three times with 10 ml of ethanol to remove the free fatty acids. In the washing, the particles were mixed with ethanol, the solution was settled by using a centrifuge, supernatant ethanol was removed and the washing procedure was repeated. Finally, the TEM analysis sample was prepared by dispersing the particles in acetone.

Printings were done using a $10'' \times 10''$ screen with 180-mesh nylon screen and an emulsion thickness of 30 µm. The printer used was a Speedline Technologies MPM Microflex screen printer (Speedline Technologies, Inc, USA). Prints with different thicknesses were made on patch antennas by multiple printings followed by drying for 15 minutes at 125°C between every printed layer. Samples for permeability measurements were prepared by printing a single layer of ink on a 0.5 mm thick piece of silicon wafer with dimensions of 10×35 mm. All printed samples were heat-treated at 125°C for 15 minutes in order to evaporate the volatiles and initialize the polymerization of the surfactant.

After electromagnetic measurements, surface profiler analysis on the printed patterns was carried out with a Dektak 8 surface profiler (Veeco Instruments Inc, USA). Finally, cross-sections of the patterns were made and optical and field emission scanning electron microscopy (FESEM) (Zeiss Ultra Plus Carl Zeiss SMT AG, Germany) was used to determine the properties of the printed patterns.

2.2. Dielectric Properties of Magnetic Ink and Related Antenna Structure

The shorted microstrip transmission-line perturbation (SMTLP) measurement technique was used to determine the complex permeability of the cobalt nanoparticle thick films [28, 30–33]. A photo of the microstrip fixture loaded with a printed film of the ink is shown in Fig. 1.

The microstrip ground and shorted planes were made of copper where one end of the microstrip line was shorted to the ground and

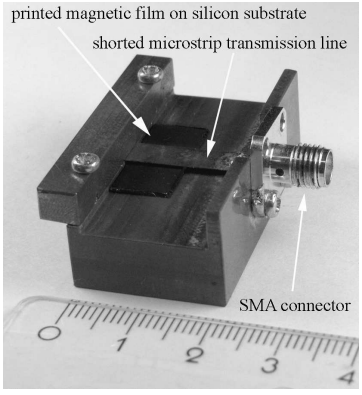

Figure 1. Shorted microstrip line fixture loaded with 13 µm printed cobalt thick film on a silicon substrate.

the other end soldered to a SubMiniature version A (SMA) coaxial connector. In the design the characteristic impedance of the microstrip line was matched to 50 Ω, i.e., the test port of the Agilent 8720ES 50 MHz to 20 GHz Network Analyzer. The width of the upper strip was 5 mm, the distance between the upper and ground plane was 1 mm and the length of the microstrip line was 20 mm. The effective complex permeability of the magnetic thick film was extracted using the SMTLP technique utilizing the measured reflection coefficients of three different samples in the fixture [28]. Measurements were made with the fixture without sample, loaded with a silicon substrate, and the same silicon substrate with a magnetic thick film printed on it.

2.3. Antenna Structure

In order to demonstrate the use of the magnetic material in the miniaturization of antennas, the concept proposed by Yang et al. [12] was partly adopted. However, instead of thin films, screen printed magnetic thick films were used for miniaturization of patch antennas. Design of the antenna is presented in Fig. 2. The antenna was modelled using Ansoft HFSS (v.13), a 3D commercial electromagnetic simulator. The square patch antenna was designed on a 1.5 mm thick FR4 substrate ($\varepsilon_r = 4.4$, $\tan\delta = 0.004$). The size of the antenna was $28 \times 28\,\text{mm}^2$ and it was fed by a quarter wavelength stub with dimensions of $0.7 \times 17\,\text{mm}^2$. The feed line width was 1.5 mm and length 10 mm, as shown in Fig. 2(a). The resonant frequency of the antenna was 2.491 GHz. In order to study the effect of the magnetic film on the antenna performance, magnetic films with different thicknesses (13–52 μm) were also modelled on top of the reference antenna to cover the fringing fields. A standard SMA connector was soldered

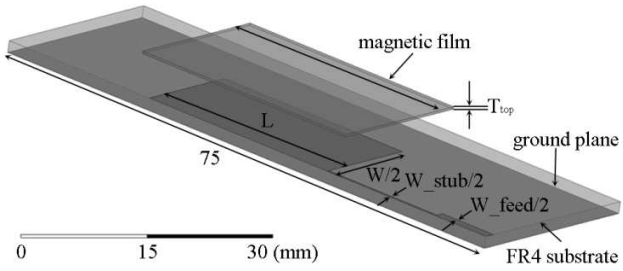

Figure 2. Schematic layout of cross section of the patch antenna loaded with magnetic thick film, $L = 28\,\text{mm}$, $W = 28\,\text{mm}$, $W\_stub = 0.7\,\text{mm}$, $W\_feed = 1.5\,\text{mm}$, $T_{top} = 13$ to $52\,\mu\text{m}$.

to the antennas for attachment of the measurement cable. A SATIMO Starlab near-field antenna measurement system was used to measure the radiation performance of the reference and printed antennas [34], starting from 800 MHz.

3. RESULTS AND DISCUSSION

3.1. TG-DSC-MS-analysis of the Ink

TG-DSC-MS analysis was carried out for the ink that was tested through printing experiments to have suitable rheological properties for printing. As shown in Figs. 3 and 4, the solvents were first evaporated from the sample at 75–200°C. Arrow (a) on Fig. 4 shows the temperature range of solvent evaporation. At higher temperatures, 380–450°C, the fatty acid surfactant/binder decomposed releasing carbon, which is clearly indicated in the ion detector signal for mass number 12 in Fig. 3. Additionally, small portion of organic material decomposes at temperature of 170°C, pointed out especially by arrow (b) on the DSC signal on Fig. 4. Arrows (a) and (b) in Fig. 3 on thermogravimetric and ion detector signals also indicate weight loss and release of carbon due to decomposition of organic material. This material is most likely to consist of unstable organic structures formed in the surfactant due to oxidative polymerization reactions occurring during the ink sample manufacture.

As a result, it was determined that the ink most suitable for

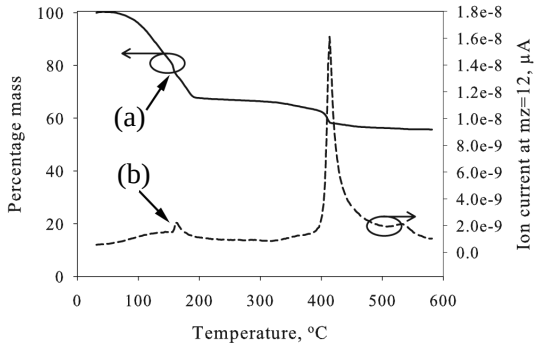

Figure 3. Thermogravimetric (solid line) and mass spectrometer data at $mz = 12$ (dashed line) of the ink sample analyzed in He atmosphere. Arrow (a) points out the loss of mass due to decomposition of organic material at temperature of 170°C, also indicated in mass spectrometer signal (Arrow (b)).

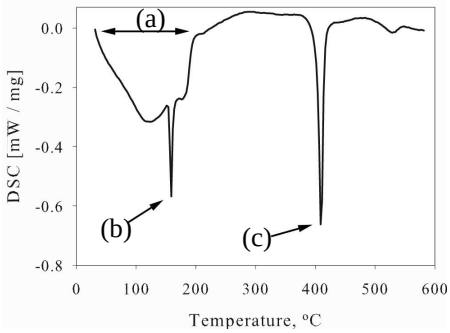

Figure 4. DSC data of the ink sample analyzed. Arrow (a) shows the temperature range of evaporation of solvents. Arrow (b) points out the consumption of energy caused by thermal decomposition of organic material indicated also by thermogravimetric and mass spectrometric measurements. Arrow (c) points to signal caused by thermal decomposition of surfactants.

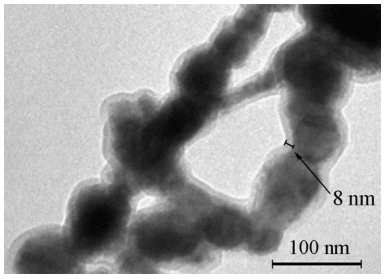

Figure 5. Cobalt nanoparticles with linoleic acid coating. Typical thickness of the organic layer was 8 nm.

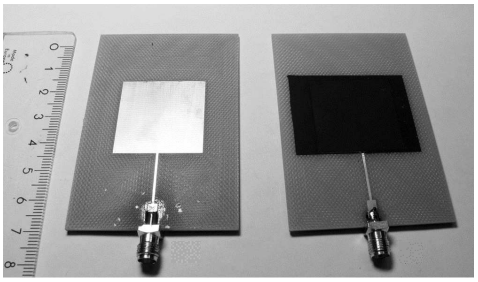

Figure 6. Photo of patch antennas: (a) reference antenna, (b) antenna loaded with magnetic thick film.

screen printing contained 34 wt.% solvents, 9.5 wt.% linoleic acid and 56.5 wt.% cobalt. Thus the dried ink contained 85.5 wt.% cobalt and 14.5 wt.% linoleic acid.

3.2. TEM Analysis of the Ink and FESEM Analysis of Printed Patterns

TEM microscopy was utilized for inspection of the linoleic acid layer applied on the cobalt nanoparticles. TEM analysis also revealed the

particles' tendency to form long chains; separate individual particles were not found, but instead the particles were in clusters or long chains forming from tens of particles. A semi-transparent 8 nm thick layer of fatty acid on the particles could be observed, as can be seen in Fig. 5.

The reference patch antenna was fabricated using the standard milling process. One to five layers of magnetic ink were printed on the radiating elements of antennas, followed by drying after each layer. The fabricated reference antenna and one with a magnetic film is shown in Fig. 6.

FESEM analyses proved that the distribution of nanoparticles in the printed patterns was homogenous. Only a few small agglomerates were visible as paler areas in the ink layer, proving that the linoleic acid acted properly as a surfactant. Also, printing experiments carried out one year later with the produced ink kept in sealed container at room temperature proved that the ink could remain non-sedimentated over a long period of time. Some minor cracks in the printed patterns were visible, indicating that a slight increase in linoleic acid content would be beneficial when especially smooth print quality is needed. Overall, it was noted that the adhesion of the ink on copper surfaces of antennas was good, as abrasive methods were needed to remove the ink. Fig. 7 presents a backscattering image from a cross-section of the patch antenna with five printed layers of ink. On the image, some cracks can be observed. However, it is likely that some of the cracks could be caused in the preparation of the FESEM samples. The separation of the ink layer from the copper layer (seen in Fig. 8) is probably caused by the polishing process of the sample.

Figure 8 shows the secondary emission image taken from the

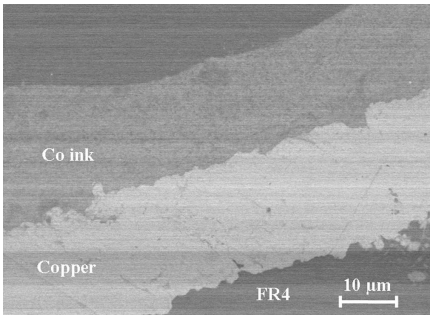

Figure 7. Backscattering image from cross-section of patch antenna with five printed layers of ink.

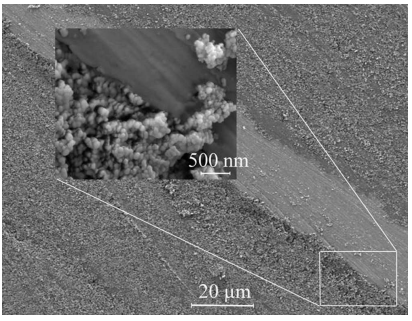

Figure 8. Secondary emission image reveals separate nanoparticles on the ink next to copper line.

printed layer on top of a patch antenna. Separate nanoparticles can be seen in the image with greater magnification. Also, homogenous dispersion of the particles can be observed.

3.3. Surface Profiler Analysis of the Printed Patterns

Surface profiler analysis results showed that the thickness of the samples varied greatly and the surface roughness of printed patterns was rather high. Thus it can be concluded that a slight increase in the amount of binding material would be beneficial to the printing characteristics. In addition to this, slower drying of the printed samples would have a positive influence on levelling the printed patterns.

Figure 9 shows the surface profiler measurements on patch antenna with one printed layer of ink. It can be observed that there is variation in thickness of the printed layer that replicates the mesh of the printing screen. This indicates that a longer levelling time prior to heat treatment would improve the print quality. The average thicknesses of the printed patterns measured with surface profiler, SEM microscopy and optical microscopy were 13, 20, 33, 39, 52 µm for 1, 2 3, 4 and 5 layers on patch antenna.

3.4. High Frequency Performance of Different Printed Patterns

Measured real and imaginary parts of the relative permeability of magnetic thick films in the frequency range from 0.2 to 5 GHz are shown in Fig. 10(a), with the addition of measured loss tangent in Fig. 10(b). The resonant behavior observed in the real and imaginary parts of the relative permeability of the magnetic thick film can be

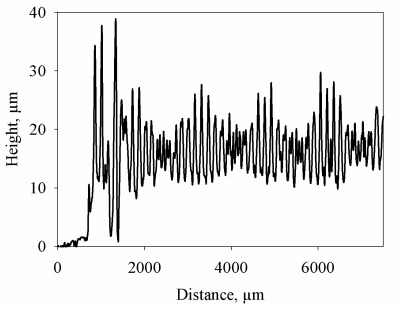

Figure 9. Measured surface profiles of magnetic films printed on patch antenna with one printed layer.

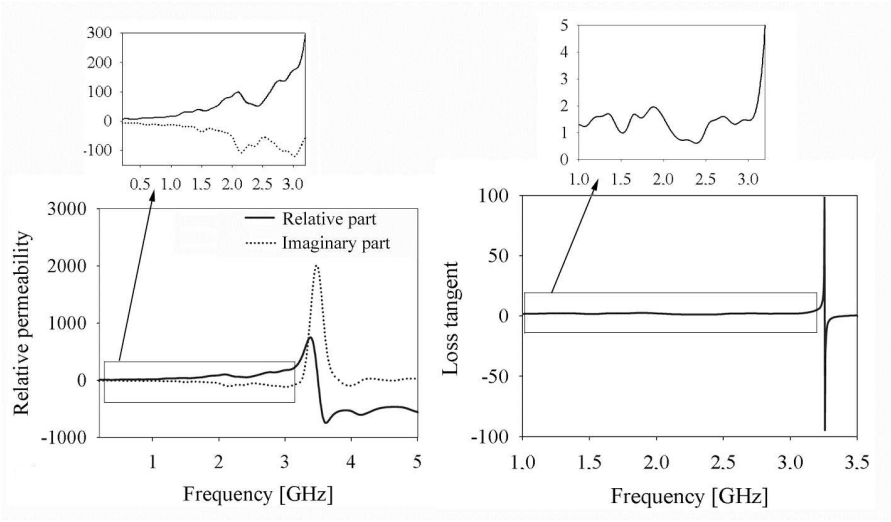

Figure 10. (a) The complex permeability of printed cobalt magnetic thick film. (b) The loss tangent of film.

attributed to the inherent ferromagnetic resonance (FMR) of the magnetic film. Similar observations have been made previously [28, 30–33]. The FMR frequency can be observed between 3 and 3.5 GHz. Measured permeability value μ_r was 81 and loss tangent $\tan\delta$ was 0.62 at 2.4 GHz frequency. The achieved permeability and loss tangent values were different compared to previous measurements carried out with ink based on cobalt nanoparticles [28], which is caused by higher metal loading of the ink and use of different surfactant and binder material in this work.

Figure 11 shows the simulated return loss of the reference and magnetic film loaded patch antennas with varied film thicknesses, respectively. The resonant frequencies of the reference patch antenna and magnetic patch antenna with 52 µm film thickness were 2.49 and 2.44 GHz. Fig. 12 shows the corresponding measured return loss of the reference and magnetic film loaded patch antennas with varied film thicknesses.

Downward shifts in resonant frequencies by 24, 34, 61, 67 and 68 MHz were measured with the printing of magnetic films of thicknesses 13, 20, 33, 39 and 52 µm onto the patch antenna, as can be seen on Fig. 12. A good agreement between the simulated and measured return loss of the antennas was observed. Loading of

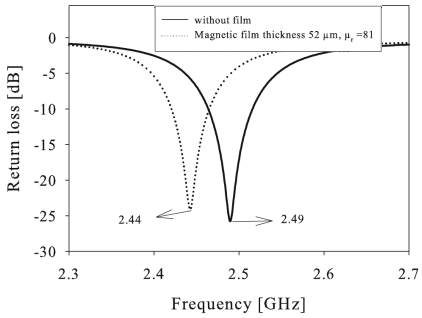

Figure 11. Simulated return loss of reference patch antenna and magnetic antenna with layer thickness 52 μm, permeability $\mu_r = 81$.

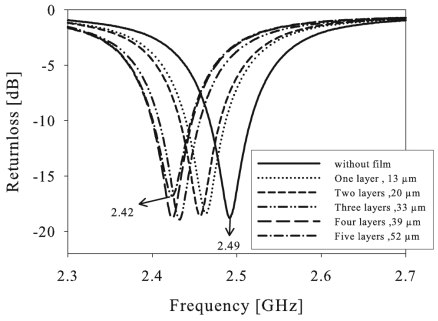

Figure 12. Measured return loss of reference patch antenna and screen printed magnetic antenna with different printed layer thickness.

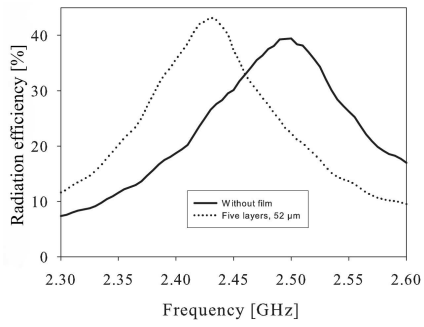

Figure 13. Measured radiation efficiencies of the reference antenna and antenna with 52 μm film thickness.

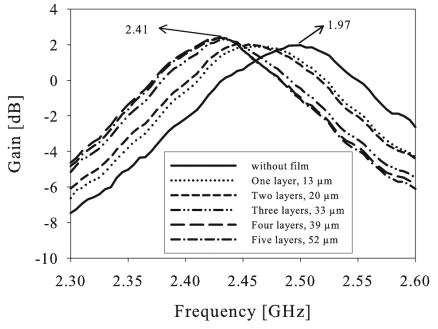

Figure 14. Measured gain of the patch antenna with different printed layer thicknesses.

magnetic cobalt films leads to wave slow down in a manner proportional to $1/\sqrt{\varepsilon_r \mu_r}$, thus leading to antenna miniaturization [35].

An increase in the film thickness leads to an increase in effective permeability of the medium loading the antenna element, thus increasing the frequency shift. A saturation in frequency shift was measured with film thicknesses over 39 μm Tunability of the resonant frequency due to magnetic film loading can be defined as,

$$\frac{f_{ref} - f_{mag}}{f_{ref}} \times 100 \tag{1}$$

where f_{ref} and f_{mag} are the resonant frequencies of the reference and magnetic film loaded antennas. Maximum tunability of 2.7% was achieved.

Figure 13 presents the measured radiation efficiency of the screen printed patch antenna with 52 µm thick magnetic film and reference antenna in the frequency range from 2.30 to 2.60 GHz. The efficiency of the patch antenna with magnetic film was 43.2%, exhibiting a higher efficiency than the reference antenna with 39.4% efficiency.

Figure 14 shows the measured total gain of the screen printed patch antennas and reference patch antenna in dB. The antenna with a screen printed magnetic film of 52 µm showed the maximum gain of 2.41 dB whereas the maximum gain for the reference antenna was 1.97 dB.

The total efficiencies, gains, frequency shifts and −10 dB bandwidths measured on antenna experiments are shown in Table 1.

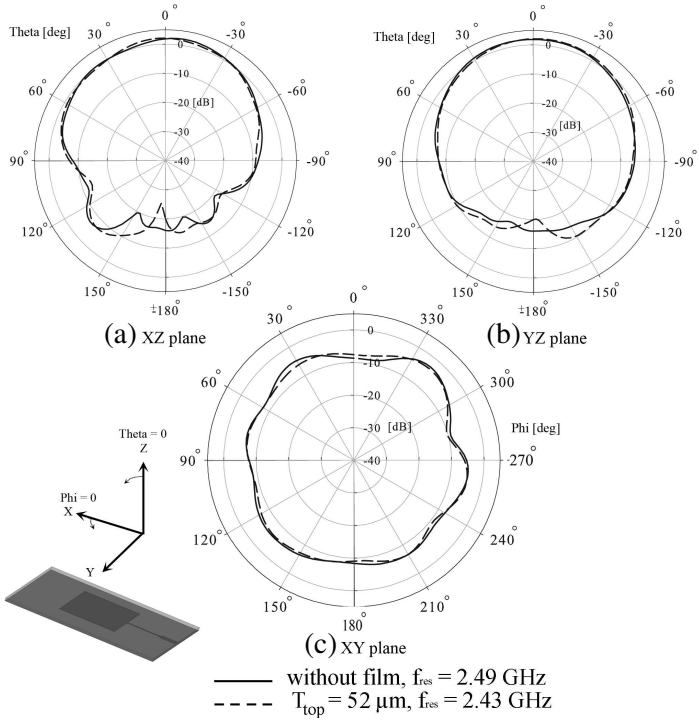

Figure 15. Measured far-field radiation patterns of the patch reference antenna and antenna with a 52 µm thick magnetic film (a) in the YZ plane, (b) in the XZ plane and (c) in the XY plane.

Table 1. Measured parameters of antenna with magnetic films.

Thickness of printed film, μm	Total efficiency, %	Gain, dB	Frequency shift, MHz	Bandwidth, MHz (−10 dB)
0	39.4	1.97	0	48.2
13	39.1	1.9	28.2	46.9
20	40.2	2.03	34.4	46.9
33	40.3	2.3	58.8	48.1
39	41.8	2.38	67.5	47.5
52	43.2	2.41	67.5	44.3

The far field radiation patterns of the patch antenna were measured using the Satimo StarLab antenna measurement system (0.8 to 6 GHz frequency range). Its main components are a vector network analyzer and probe array controller. With StarLab the DUT is placed at the center of the support structure and measurements are made by electronically scanning the probe array. The measured far-field radiation patterns of the patch reference antenna and antenna with a 52 μm screen printed magnetic thick film are presented in Fig. 15. The patch antenna showed maximum gain in the XZ and YZ planes. The effect of the magnetic film on the shapes of the radiation patterns was found to be minimal.

4. CONCLUSION

Screen printed, low temperature cured magnetic cobalt nanoparticle films have been introduced to tune the resonant frequencies of patch antennas. Measurements on magnetic patch antennas showed that the resonant frequency (2.49 GHz) can be decreased by 68 MHz with a 52 μm thick film, indicating that these films are potential candidates for the miniaturization of cost effective and mass producible antennas for mobile terminal applications. Antennas loaded with screen printed cobalt thick films could be miniaturized without compromising antenna efficiencies and without any significant distortion in the shapes of the radiation patterns.

In order to avoid the formation of cracks in the printed films, the curing process of the ink should be further optimized. However, it was observed that despite the cracks in printed films, the adhesion of the ink to the metallic surfaces on the antennas was good due to covalent bonding between the copper surface of the antenna and the

carboxylic acid parts of linoleic acid. Furthermore, the ink exhibited good stability as no sedimentation of the particles in the ink was observed in cross-section samples of the printed patterns. Also, the ink samples remained printable after one year of storage in a sealed container at room temperature.

This method of antenna miniaturization would be useful also on other antenna types such as dual-band monopole antennas, planar inverted-F antennas and loop antennas. The antennas could be further miniaturized in some extent by increasing the nanoparticle loading of the ink, although this loading level is the highest achievable with linoleic acid. Also the required amount of the ink could be reduced by printing it only onto areas on the antenna element with high surface currents.

ACKNOWLEDGMENT

Authors A. S. and M. N. acknowledge the Riitta and Jorma Takanen foundation for financial support of the work.

REFERENCES

1. Lee, B. and F. J. Harackiewicz, "Miniature microstrip antenna with a partially filled high-permittivity substrate," *IEEE Transactions on Antennas and Propagation*, Vol. 50, No. 8, 1160–1162, 2002.
2. Kula, J. S., D. Psychoudakis, W. J. Liao, C. C. Chen, J. L. Volakis, and J. W. Halloran, "Patch-antenna miniaturization using recently available ceramic substrates," *IEEE Antennas and Propagation Magazine*, Vol. 48, No. 6, 13–20, 2006.
3. Volakis, J. L., *Antenna Engineering Handbook*, 4th Edtion, Vol. 7, 3–4, The McGraw Hill Companies, 2007.
4. Jackson, D. and N. Alexopoulos, "Gain enhancement methods for printed circuit antennas," *IEEE Transactions on Antennas and Propagation*, Vol. 33, No. 9, 976–987, 1985.
5. Mosallaei, H. and K. Sarabandi, "Antenna miniaturization and bandwidth enhancement using a reactive impedance substrate," *IEEE Transactions on Antennas and Propagation*, Vol. 52, No. 9, 2403–2414, 2004.
6. Rainville, P. J. and F. J. Harackiewicz, "Magnetic tuning of a microstrip patch antenna fabricated on a ferrite film," *IEEE Microwave and Guided Wave Letters*, Vol. 2, No. 12, 483–485, 1992.

7. Brown, A. D., J. L. Volakis, L. C. Kempel, and Y. Botros, "Patch antennas on ferromagnetic substrates," *IEEE Transactions on Antennas and Propagation*, Vol. 47, No. 1, 26–32, 1999.
8. Do, T. B. and J. W. Halloran, "Fabrication of polymer magnetics," *IEEE Antennas and Propagation Society International Symposium*, 1709–1712, 2007.
9. Volakis, J. L. and C. Chen, "Miniaturization and materials in antenna design," *IDGA's Military Antennas 2007 Conference*, Washington DC, Sep. 2007.
10. Chikazumi, S., *Physics of Magnetism*, Krieger Publishing Company, 1978.
11. Sun, N. X., J. W. Wang, A. Daigle, C. Pettiford, H. Mosallaei, and C. Vittoria, "Electronically tunable magnetic patch antennas with metal magnetic films," *Electronics Letters*, Vol. 43, No. 8, 434–436, 2007.
12. Yang, G. M., A. Daigle, M. Liu, O. Obi, S. Stoute, K. Naishadham, and N. X. Sun, "Planar circular loop antennas with self-biased magnetic film loading," *IEEE Antennas and Propagation Society International Symposium, AP-S 2008*, 1–4, 2008.
13. Yang, G. M., X. Xing, A. Daigle, M. Liu, O. Obi, S. Stoute, K. Naishadham, and N. X. Sun, "Tunable miniaturized patch antennas with self-biased multilayer magnetic films," *IEEE Transactions on Antennas and Propagation*, Vol. 57, No. 7, 2190–2192, 2009.
14. Rao, C. R. K. and D. C. Trivedi, "Biphasic synthesis of fatty acids stabilized silver nanoparticles: Role of experimental conditions on particle size," *Mater. Chem. Phys.*, Vol. 99, No. 2–3, 354–360, 2006.
15. Bell, N. S., M. E. Schendel, and M. Piech, "Rheological properties of nanopowder alumina coated with adsorbed fatty acids," *J. Colloid Interface Sci.*, Vol. 287, No. 1, 94–106, 2005.
16. Lan, Q., C. Liu, F. Yang, S. Liu, J. Xu, and D. Sun, "Synthesis of bilayer oleic acid-coated Fe_3O_4 nanoparticles and their application in pH-responsive pickering emulsions," *J. Colloid Interface Sci.*, Vol. 310, No. 1, 260–269, 2007.
17. Sailer, R. A. and M. D. Soucek, "Investigation of cobalt drier retardation," *European Polymer Journal*, Vol. 36, No. 4, 803–811, 2000.
18. Yang, T., R. N. C. Brown, L. C. Kempel, and P. Kofinas, "Surfactant-modified nickel zinc iron oxide/polymer nanocompos-

ites for radio frequency applications," *Journal of Nanoparticle Research,* Vol. 12, No. 8, 2967–2978, 2010.

19. Moser, A., K. Takano, D. T. Margulies, M. Albrecht, Y. Sonobe, Y. Ikeda, S. Sun, and E. E. Fullerton, "Magnetic recording: Advancing into the future," *J. Phys. D*, Vol. 35, No. 19, R157–R167, 2002.
20. Bigioni, T. P., X. Lin, T. T. Nguyen, E. I. Corwin, T. A. Witten, and H. M. Jaeger, "Kinetically driven self assembly of highly ordered nanoparticle monolayers," *Nature Materials*, Vol. 5, No. 4, 265–270, 2006.
21. Rudenkiy, S., M. Frerichs, F. Voigts, W. Maus-Friedrichs, V. Kempter, R. Brinkmann, N. Matoussevitch, W. Brijoux, H. Bönnemann, N. Palina, and H. Modrow, "Study of the structure and stability of cobalt nanoparticles for ferrofluidic applications," *Applied Organometallic Chemistry*, Vol. 18, No. 10, 553–560, 2004.
22. Mornet, S., S. Vasseur, F. Grasset, and E. Duguet, "Magnetic nanoparticle design for medical diagnosis and therapy," *Journal of Materials Chemistry*, Vol. 14, No. 14, 2161–2175, 2004.
23. Neuberger, T., B. Schöpf, H. Hofmann, M. Hofmann, and B. Von Rechenberg, "Superparamagnetic nanoparticles for biomedical applications: Possibilities and limitations of a new drug delivery system," *J. Magn. Mater.*, Vol. 293, No. 1, 483–496, 2005.
24. Hu, A., G. T. Yee, and W. Lin, "Magnetically recoverable chiral catalysts immobilized on magnetite nanoparticles for asymmetric hydrogenation of aromatic ketones," *J. Am. Chem. Soc.*, Vol. 127, No. 36, 12486–12487, 2005.
25. Pohjalainen, E., M. Pohjakallio, C. Johans, K. Kontturi, J. V. I. Timonen, O. Ikkala, R. H. A. Ras, T. Viitala, M. T. Heino, and E. T. Seppälä, "Cobalt nanoparticle langmuir-schaefer films on ethylene glycol subphase," *Langmuir*, Vol. 26, No. 17, 13937–13943, 2010.
26. Aleksandrovic, V., D. Greshnykh, I. Randjelovic, A. Frömsdorf, A. Kornowski, S. V. Roth, C. Klinke, and H. Weller, "Preparation and electrical properties of cobalt-platinum nanoparticle monolayers deposited by the langmuir-blodgett technique," *ACS Nano*, Vol. 2, No. 6, 1123–1130, 2008.
27. Ago, H., J. Qi, K. Tsukagoshi, K. Murata, S. Ohshima, Y. Aoyagi, and M. Yumura, "Catalytic growth of carbon nanotubes and their patterning based on ink-jet and lithographic techniques," *J. Electroanal. Chem.*, Vol. 559, 25–30, 2003.

28. Nelo, M., A. K. Sowpati, V. K. Palukuru, J. Juuti, and H. Jantunen, "Formulation of screen printable cobalt nanoparticle ink for high frequency applications," *Progress In Electromagnetics Research*, Vol. 110, 253–266, 2010.
29. Xanthos, M., *Functional Fillers for Plastics*, 2nd edtion, 119, Viley-Verlag GMBH, 2010.
30. Wu, Y., Z.-X. Tang, Y. Xu, and B. Zhang, "Measure the complex permeability of ferromagnetic thin films: Comparison shorted microstrip method with microstrip transmission method," *Progress In Electromagnetics Research Letters*, Vol. 11, 173–181, 2009.
31. Liu, Y., L. Chen, C. Y. Tan, H. J. Liu, and C. K. Ong, "Broadband complex permeability characterization of magnetic thin films using shorted microstrip transmission-line perturbation," *Rev. Sci. Instrum.*, Vol. 76, No. 6, 2005.
32. Wu, Y., Z. Tang, Y. Xu, B. Zhang, and X. He, "Measuring complex permeability of ferromagnetic thin film up to 10 GHz," *Progress In Electromagnetics Research Letters*, Vol. 9, 139–145, 2009.
33. Wu, Y., Z. Tang, Y. Xu, B. Zhang, and H. Xi, "A new shorted microstrip method to determine the complex permeability of thin films," *IEEE Transactions on Magnetics*, Vol. 46, No. 3, 886–888, 2010.
34. Iversen, P. O., P. Garreau, and D. Burrell, "Real-time spherical near-field handset antenna measurements," *IEEE Antennas and Propagation Magazine*, Vol. 43, No. 3, 90–94, 2001.
35. Volakis, J. L., C. C. Chen, and K. Fujimoto, *Small Antennas Miniaturization Techniques & Applications*, 160, The McGraw. Hill Companies, 2010.